Modeling, Estimation, and Bounds for Precision Two-way Time Transfer and Ranging

Patrick Bidigare, Charlie Obranovich, David Raeman, Dan Chang
Synoptic Engineering
Arlington, VA 22201
{patrick,charlie,david,dan}@synopticengineering.com

D. Richard Brown III
Electrical and Computer Engineering Department
Worcester Polytechnic Institute
Worcester, MA 01609 USA
drb@wpi.edu

Abstract— **Over-the-air precision two-way time transfer and ranging (PTTR) uses the signals exchanged between two RF transceivers to estimate the range between them and the offset between their clocks. Our paper makes three significant contributions to the estimation and position, navigation, and timing literature. First, we introduce a propagation channel model characterized by its amplitude (attenuation), phase shift, and propagation delay. This three-parameter formulation is quite practical for modeling signal exchange over line-of-sight channels with arbitrary additive wide-sense stationary noise that also captures electronic effects. Second, we derive the Cramer-Rao Lower Bound (CRLB) for this three parameter channel model. We show that there is a canonical definition of phase shift for which the CRLB is a diagonal matrix. The derived CRLB depends on simple properties of the signal and noise power spectral density (PSD) related to whitened bandwidth and whitened center frequency as well as the signal to noise ratio. Third, we derive a maximum likelihood estimator (MLE) for the amplitude, phase shift, and delay given the reference waveform, received waveform samples, and noise PSD. A novel aspect of the derived MLE is that it is implemented entirely in the frequency domain, which makes the MLE more computationally efficient than a typical time-domain implementation. Using an example reference waveform, we show that the derived MLE achieves an empirical covariance close to the CRLB for sufficiently high signal to noise ratios. The estimation results of our paper are directly relevant to over-the-air PTTR applications operating in direct-path, line-of-sight propagation environments. The generality of the waveform and noise formulations allow our estimator and bounds to be applied to arbitrary PTTR ranging waveforms in colored interference environments. We present a system architecture utilizing this estimator that enables PTTR on existing wireless networks with no changes to the communications protocol or radio hardware or software.**

TABLE OF CONTENTS

Proc. IEEE Aerospace Conf, Big Sky, MT, March 2022.

1. INTRODUCTION

Applications

Precision two-way time transfer and ranging (PTTR) using RF communication signals has many applications in navigation and environmental sensing. Inter-radio ranges obtained from a wireless network can be used to establish the three-dimensional locations of the radios in a network-centric coordinate system that is uniquely determined up to translations and rotations (Fig. 1). The precision available with our

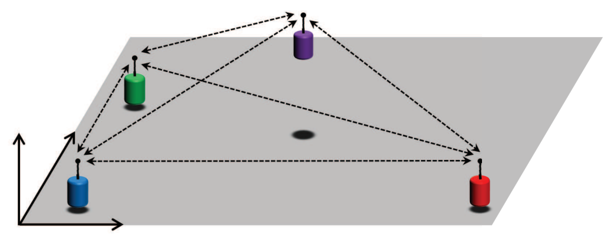

Figure 1. PTTR enables GPS-free navigation.

PTTR using RF communications can also be utilized to make very fine measurements of propagation delay changes due to changes in atmospheric refractivity. Since phase delay measurements are sensitive to time delay changes on the scale of the carrier period, these measurements can be used to infer small scale changes in temperature, atmospheric pressure and water vapor pressure that affect the refractive index of the atmosphere. This feature makes PTTR-derived propagation delays potentially valuable for weather and climate applications.

Prior Work

A key component of any two-way time transfer and ranging system, e.g., [1–6], is accurate time delay estimation. Fundamental limitations of time delay estimation for narrow-band and wide-band signals were studied in [7] and [8], respectively. The analysis in [7, 8] focused primarily on deriving bounds for the accuracy of time delay estimation for spectrally flat *bandpass* signals with constant signal-to-noise ratio (SNR) over the band of interest. Weiss and Weinstein derived several elegant results including SNR thresholds that divide passive time delay estimation performance into distinct operating regimes including an "ambiguity-dominated" regime with performance governed by the Barankin bound at moderate SNRs and an "ambiguity-free" regime with performance governed by the Cramer-Rao lower bound at high

SNRs. This work was generalized to "split bandpass" signals and a maximum likelihood estimator was developed for these types of signals in [9].

The radar literature, e.g., [10, 11], has also considered the classical problem of time delay estimation. This body of literature typically considers delay estimation of signals with general frequency-domain representation $B(\omega)$ rather than signals with specific power spectra as in [7–9]. A well-known result from the radar literature states that the variance of time delay estimates is lower bounded by

$$\mathrm{var}(\hat{\tau}) \geq \frac{1}{2\beta^2\rho} \tag{1}$$

where ρ is the post-integration SNR at the receiver and

$$\beta^2 = \frac{\int_{-\infty}^{\infty} (\omega - \langle\omega\rangle)^2 \, B(\omega)|^2 \, df}{\int_{-\infty}^{\infty} |B(\omega)|^2 \, df} \tag{2}$$

is the mean square bandwidth of $B(\omega)$ where

$$\langle\omega\rangle = \int_{-\infty}^{\infty} \omega B(\omega) \, d\omega \tag{3}$$

denotes the mean frequency of the signal $B(\omega)$ [12]. The radar literature typically assumes $\langle\omega\rangle = 0$, although we do not make that assumption here. The bound in (1) can be shown to be consistent with the Barankin bound in [7, 8] for post-integration SNRs in the ambiguity-dominated regime.

This paper considers a further generalization of the types of signals used for delay estimation by considering a scenario in which, like the radar literature, the signal of interest is general, but unlike the prior literature, the received signal has two additional nuisance parameters: an unknown phase offset due to electronic effects in the transceivers and an unknown received amplitude due to propagation and electronic effects at the transceivers. This three-parameter channel model is practical for modeling signal exchange over line-of-sight channels with arbitrary additive wide-sense stationary noise that also captures electronic effects in the transceivers. In addition to deriving fundamental lower bounds for the variance of the delay, phase, and amplitude estimates, we also develop a computationally efficient maximum likelihood estimator (MLE) for the delay, phase, and amplitude given the reference waveform, received waveform samples, and noise power spectral density.

The parsimonious channel model, fundamental bounds, and computationally-efficient algorithm for estimating the channel amplitude, delay and phase shift for arbitrary signals represent a significant advance over the prior literature as it incorporates practical transceiver considerations not considered in the previous work.

2. Timing and Ranging from Wireless Networks

Wireless communications networks use over-the-air exchange of signals between radios to pass information. From the perspective of the communication application, the clock offset and propagation delay represent nuisance effects that must be compensated for, however careful measurement of these parameters allows the signals that are normally transmitted across the network to be used as an organic source of time synchronization and ranging in precision navigation and timing applications where other sources of localization and time synchronization, such as GNSS, are unavailable. Synoptic Engineering is developing a method for estimating

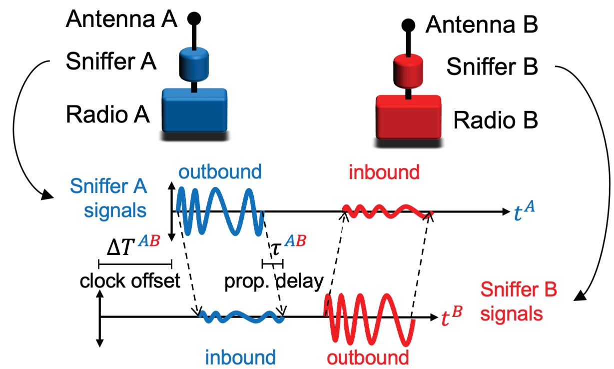

Figure 2. Timing and ranging architecture.

organic time synchronization and inter-radio ranges by inserting RF "sniffers" in-line between existing time-duplexed wireless networking radios and their antennas (Fig. 2 top). These sniffers record both the outbound signals generated by their attached radios and the inbound signals received over the antenna from neighboring radios (Fig. 2 bottom). An pristine outbound signal (blue) generated from Radio A will be collected by Sniffer A and later seen as a noisy attenuated, phase-shifted and delayed inbound signal by Sniffer B. Since sniffers A and B each maintain their own local timebases, the apparent offset, called a pseudorange in the GPS vernacular, will be the sum of the propagation time τ^{AB} and clock offset ΔT^{AB}. When Radio B transmits, its communication signal will be seen as a pristine outbound signal (red) at Sniffer B and later as a noisy, phase-shifted and delayed inbound signal by Sniffer A, however in this direction, the pseudorange will be the difference $\tau^{AB} - \Delta T^{AB}$. The reciprocal nature of propagation and the anti-reciprocal nature of change-of-timebase allow these quantities to be independently estimated when the recorded signals from both sniffers are shared over a network. A Kalman Filter allows the dynamic quantities of clock offset and range to be tracked using pseudoranges as measurement updates.

The elegance of this approach is that no modifications are needed to the waveforms or radios and it applies to any time-duplexed two-way wireless communication system operating in line-of-sight propagation conditions, however it requires that we develop a delay estimator to measured the apparent offsets between outbound and inbound copies of the waveform that works with arbitrary communications waveforms in additive colored noise. The remainder of the paper develops such an estimator and lower-bounds its performance.

3. System Model

In this paper, we assume a linear time invariant channel $h(t)$ with frequency response $H(\omega)$. We further assume $H(\omega)$ is well approximated by a constant envelope and affine phase over the band of interest as shown in Fig. 3. In the modulated signal spectrum band of support, the signal experiences a group delay of $\tau = -\frac{dH(\omega)}{d\omega}$ seconds and an additional phase shift of ϕ radians as shown in Fig. 3.

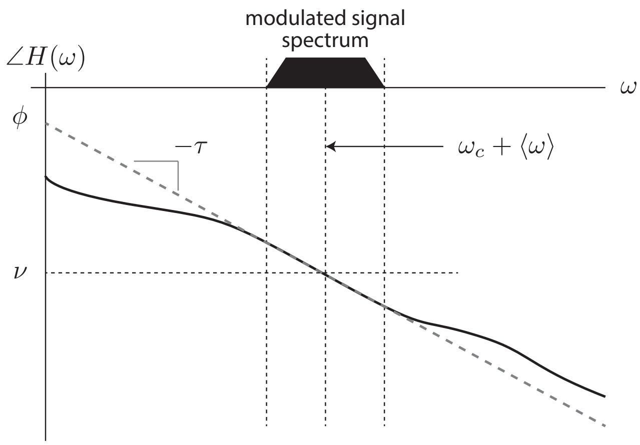

Figure 3. Affine channel model.

We assume the modulated signal is a baseband signal $\tilde{b}(t)$ modulated by a carrier at frequency f_c Hertz. Letting $\omega_c = 2\pi f_c$ for notational convenience, the continuous time received signal after propagation through the channel $h(t)$ and demodulation at the receiving node can be written as

$$\tilde{r}(t) = ae^{j\phi}\tilde{b}(t-\tau)\exp(-j\omega_c\tau) + \tilde{n}(t) \tag{4}$$

where the amplitude $a > 0$ and phase $\phi \in [-\pi, \pi)$ are assumed to be both unknown and $n(t)$ is complex additive Gaussian noise. Both $\tilde{b}(t)$ and ω_c are assumed to be known.

This three-parameter formulation is quite practical for modeling signal exchange with real transceivers because, while a delay always causes a phase shift, not every phase shift corresponds to a delay. For example, transceiver electronics may cause fixed phase shifts without corresponding delays. Previous results have considered only one- or two-parameter channel models (delay, amplitude + phase, amplitude + delay) and have not addressed the general wide-sense stationary Gaussian noise that our model considers.

Assuming a sampling period of T and first sample time of t_0, the sampled received signal can be written as

$$\begin{aligned}\tilde{r}_k &= \tilde{r}(t_0 + kT) \\ &= ae^{j\phi}\tilde{b}(t_0 + kT - \tau)\exp(-j\omega_c\tau) + n(t_0 + kT) \\ &= a\tilde{b}_k(\tau)\exp(-j(\omega_c\tau - \phi)) + \tilde{n}_k\end{aligned}$$

for samples $k = 0, \ldots, N-1$. We can vectorize the observation as

$$\tilde{\boldsymbol{r}} = a\exp(-j(\omega_c\tau - \phi))\underbrace{\begin{bmatrix}\tilde{b}_0(\tau) \\ \vdots \\ \tilde{b}_{N-1}(\tau)\end{bmatrix}}_{\tilde{\boldsymbol{b}}(\tau)} + \tilde{\boldsymbol{n}}$$

where $\tilde{\boldsymbol{b}}(\tau) : \mathbb{R} \mapsto \mathbb{R}^{\mathbb{N}}$ is a vector of time-shifted samples of the continuous-time baseband signal $\tilde{b}(t)$.

We assume the noise is distributed as $\tilde{\boldsymbol{n}} \sim \mathcal{CN}(0, \boldsymbol{C})$ where $\mathcal{CN}$ denotes the proper complex Gaussian distribution and the positive definite covariance $\boldsymbol{C}$ is known. Since $\boldsymbol{C}$ is positive definite, $\boldsymbol{C}^{-1}$ is also positive definite. Hence, we can denote $\boldsymbol{C}^{-1} = \boldsymbol{D}^\top\boldsymbol{D}$, where $\boldsymbol{D}$ can be computed with via a Cholesky factorization [13]. Letting

$$\begin{aligned}\boldsymbol{r} &= \boldsymbol{D}\tilde{\boldsymbol{r}} \\ &= a\exp(-j(\omega_c\tau - \phi))\boldsymbol{b}(\tau) + \boldsymbol{n}\end{aligned}$$

where $\boldsymbol{b}(\tau) = \boldsymbol{D}\tilde{\boldsymbol{b}}(\tau)$ and $\boldsymbol{n} = \boldsymbol{D}\tilde{\boldsymbol{n}}$. Note that $\boldsymbol{n} \sim \mathcal{CN}(0, \boldsymbol{I})$, i.e., the coordinate transformation $\boldsymbol{r} = \boldsymbol{D}\tilde{\boldsymbol{r}}$ whitened and normalized the noise such that $\mathrm{var}(n_k) = 1$.

4. Lower Bounds on Parameter Estimation Accuracy

This section derives closed form expressions for the Cramer-Rao lower bound for the estimation of the unknown parameters τ, a, and ϕ. Unlike the prior literature, e.g., Weiss and Weinstein 1983 which assumed specific narrowband signal models, we make no assumptions about the waveform exchanged between the two RF transceivers.

We denote the unknown parameter vector as $\boldsymbol{\theta} = [\tau, a, \phi]^\top$. Note that the whitened observation $\boldsymbol{r} \sim \mathcal{CN}(\boldsymbol{\mu}(\boldsymbol{\theta}), \boldsymbol{I})$ where

$$\boldsymbol{\mu}(\boldsymbol{\theta}) = a\exp(-j(\omega_c\tau - \phi))\boldsymbol{b}(\tau).$$

From [14, p. 524], we can write the jointly Gaussian whitened observation's density as

$$p(\boldsymbol{r}; \boldsymbol{\theta}) = \frac{1}{\pi^N}\exp\left(-(\boldsymbol{r} - \boldsymbol{\mu}(\boldsymbol{\theta}))^H(\boldsymbol{r} - \boldsymbol{\mu}(\boldsymbol{\theta}))\right).$$

Also, from [14], the elements of the Fisher information matrix can be calculated by computing

$$I_{\ell,m} = 2\mathrm{Re}\left(\frac{\partial\boldsymbol{\mu}^H(\boldsymbol{\theta})}{\partial\theta_\ell} \cdot \frac{\partial\boldsymbol{\mu}(\boldsymbol{\theta})}{\partial\theta_m}\right).$$

The partial derivative with respect to τ can be computed as

$$\frac{\partial\boldsymbol{\mu}(\boldsymbol{\theta})}{\partial\tau} = -ja\exp(-j(\omega_c\tau - \phi))\left(\mathcal{W}\boldsymbol{b}(\tau) + \omega_c\boldsymbol{b}(\tau)\right)$$

where $\mathcal{W} := \frac{1}{j}\frac{\partial}{\partial t} = -\frac{1}{j}\frac{\partial}{\partial\tau}$ is the "frequency operator" defined in [12, p. 11]. The partial derivative with respect to a can be computed as

$$\frac{\partial\boldsymbol{\mu}(\boldsymbol{\theta})}{\partial a} = \exp(-j(\omega_c\tau - \phi))\boldsymbol{b}(\tau)$$

and the partial derivative with respect to ϕ can be computed as

$$\frac{\partial\boldsymbol{\mu}(\boldsymbol{\theta})}{\partial\phi} = ja\exp(-j(\omega_c\tau - \phi))\boldsymbol{b}(\tau)$$

Fisher Information Matrix and Cramer Rao Lower Bound

The $(1,1)$ element of the Fisher information matrix can be computed as

$$I_{1,1} = 2a^2\left(\mathcal{W}\boldsymbol{b}(\tau) + \omega_c\boldsymbol{b}(\tau)\right)^H\left(\mathcal{W}\boldsymbol{b}(\tau) + \omega_c\boldsymbol{b}(\tau)\right)$$

There are four terms

$$\begin{aligned} T_1 &= 2a^2 \left(\mathcal{W}\boldsymbol{b}(\tau)\right)^H \left(\mathcal{W}\boldsymbol{b}(\tau)\right) \\ T_2 &= 2a^2\omega_c \left(\mathcal{W}\boldsymbol{b}(\tau)\right)^H \boldsymbol{b}(\tau) \\ T_3 &= 2a^2\omega_c \boldsymbol{b}^H(\tau)\mathcal{W}\boldsymbol{b}(\tau) \\ T_4 &= 2a^2\omega_c^2 \boldsymbol{b}^H(\tau)\boldsymbol{b}(\tau). \end{aligned}$$

Assuming the observation is long enough so that the entire whitened baseband pulse $b(t-\tau)$ is captured in the observation, we can write

$$\begin{aligned} \left(\mathcal{W}\boldsymbol{b}(\tau)\right)^H \left(\mathcal{W}\boldsymbol{b}(\tau)\right) &= \left(\frac{1}{j}\frac{\partial}{\partial t}\boldsymbol{b}(\tau)\right)^H \left(\frac{1}{j}\frac{\partial}{\partial t}\boldsymbol{b}(\tau)\right) \\ &\approx \frac{1}{T}\int \left|\frac{\partial}{\partial t}b(t)\right|^2 dt \\ &= \langle\omega^2\rangle \frac{1}{T}\int |b(t)|^2\, dt \\ &\approx \langle\omega^2\rangle \boldsymbol{b}^H(\tau)\boldsymbol{b}(\tau) \end{aligned}$$

where $\langle\omega^2\rangle$ is the mean square frequency of the whitened baseband pulse $b(t)$. The second equality follows [12], the approximations occur in the substitution of the integrals for the inner products where we have used the fact that

$$\frac{\partial}{\partial \tau}b(t-\tau) = -\frac{\partial}{\partial t}b(t-\tau).$$

We define

$$\mathcal{E}_b = \boldsymbol{b}^H(\tau)\boldsymbol{b}(\tau) \tag{5}$$

which is the energy in the vector of reference samples. This quantity is independent of τ because time translation does not affect energy.

Also from [12], we can write

$$\begin{aligned} T_3 &= 2a^2\omega_c \boldsymbol{b}^H(\tau)\mathcal{W}\boldsymbol{b}(\tau) \\ &= 2a^2\omega_c\langle\omega\rangle\mathcal{E}_b \end{aligned}$$

where $\langle\omega\rangle$ is the mean frequency of the whitened baseband pulse. It is straightforward to show that $T_2 = T_3$. Finally,

$$\begin{aligned} T_4 &= 2a^2\omega_c^2\|\boldsymbol{b}(\tau)\|^2 \\ &= 2a^2\omega_c^2\mathcal{E}_b. \end{aligned}$$

Putting it all together, we have

$$\begin{aligned} I_{1,1} &= 2a^2\mathcal{E}_b\left(\langle\omega^2\rangle + 2\omega_c\langle\omega\rangle + \omega_c^2\right) \\ &= 2a^2\mathcal{E}_b\Big\langle(\omega+\omega_c)^2\Big\rangle \end{aligned}$$

where $\Big\langle(\omega+\omega_c)^2\Big\rangle$ is the mean square frequency of the whitened modulated signal.

Next, we turn our attention to the $(2,2)$ element of the Fisher information matrix. We can compute

$$\begin{aligned} I_{2,2} &= 2\boldsymbol{b}^H(\tau)\boldsymbol{b}(\tau) \\ &= 2\mathcal{E}_b. \end{aligned}$$

For the $(3,3)$ element of the Fisher information matrix, we can compute

$$\begin{aligned} I_{3,3} &= 2a^2\boldsymbol{b}^H(\tau)\boldsymbol{b}(\tau) \\ &= 2a^2\mathcal{E}_b. \end{aligned}$$

It is easy to see that the Fisher information matrix elements $(1,2)$, $(2,1)$, $(2,3)$, and $(3,1)$ are all zero since the product of the partial derivatives in (5) is purely imaginary.

The remaining Fisher information matrix elements are the $(1,3)$ and $(3,1)$ elements. Under the current parameterization, these are non-zero and can be calculated as

$$\begin{aligned} I_{3,1} &= 2\mathrm{Re}\left(\frac{\partial\boldsymbol{\mu}^H(\boldsymbol{\theta})}{\partial\phi}\frac{\partial\boldsymbol{\mu}(\boldsymbol{\theta})}{\partial\tau}\right) \\ &= -2a^2\boldsymbol{b}^H(\tau)(\mathcal{W}\boldsymbol{b}(\tau) + \omega_c\boldsymbol{b}(\tau)) \\ &= -2a^2\mathcal{E}_b\left(\langle\omega\rangle + \omega_c\right) \\ &= -2a^2\mathcal{E}_b\Big\langle\omega+\omega_c\Big\rangle. \end{aligned}$$

We now summarize these results. Denote by

$$\rho = a^2\mathcal{E}_b \tag{6}$$

the integrated signal to noise ratio (SNR) and let $\tilde{\omega} = \omega + \omega_c$ represent the frequencies of the (whitened) bandpass signal. We can then write the Fisher information matrix as

$$\boldsymbol{I} = \begin{bmatrix} 2\rho\langle\tilde{\omega}^2\rangle & 0 & -2\rho\langle\tilde{\omega}\rangle \\ 0 & 2\mathcal{E}_b & 0 \\ -2\rho\langle\tilde{\omega}\rangle & 0 & 2\rho \end{bmatrix}. \tag{7}$$

The Cramer-Rao lower bound is the inverse of the Fisher information matrix. This can be computed as

$$\boldsymbol{I}^{-1} = \begin{bmatrix} \frac{1}{2\rho\left(\langle\tilde{\omega}^2\rangle - \langle\tilde{\omega}\rangle^2\right)} & 0 & \frac{\langle\tilde{\omega}\rangle}{2\rho\left(\langle\tilde{\omega}^2\rangle - \langle\tilde{\omega}\rangle^2\right)} \\ 0 & \frac{1}{2\mathcal{E}_b} & 0 \\ \frac{\langle\tilde{\omega}\rangle}{2\rho\left(\langle\tilde{\omega}^2\rangle - \langle\tilde{\omega}\rangle^2\right)} & 0 & \frac{\langle\tilde{\omega}^2\rangle}{2\rho\left(\langle\tilde{\omega}^2\rangle - \langle\tilde{\omega}\rangle^2\right)} \end{bmatrix}.$$

Note that

$$\begin{aligned} \langle\tilde{\omega}^2\rangle - \langle\tilde{\omega}\rangle^2 &= \langle(\omega_c+\omega)^2\rangle - \langle\omega_c+\omega\rangle^2 \\ &= \omega_c^2 + 2\omega_c\langle\omega\rangle + \langle\omega^2\rangle - \Big(\omega_c^2 + 2\omega_c\langle\omega\rangle + \langle\omega\rangle^2\Big) \\ &= \langle\omega^2\rangle - \langle\omega\rangle^2 \\ &= \beta^2 \end{aligned}$$

where β^2 is the mean square bandwidth defined in (2). Hence the CRLB can also be written as

$$\mathrm{cov}\left[\hat{\boldsymbol{\theta}}\right] \geq \boldsymbol{I}^{-1} = \begin{bmatrix} \frac{1}{2\rho\beta^2} & 0 & \frac{\langle\tilde{\omega}\rangle}{2\beta^2)} \\ 0 & \frac{1}{2\mathcal{E}_b} & 0 \\ \frac{\langle\tilde{\omega}\rangle}{2\rho\beta^2} & 0 & \frac{\langle\tilde{\omega}^2\rangle}{2\rho\beta^2} \end{bmatrix}. \tag{8}$$

Note that the (1,1) element is consistent with the bound in (1) from the radar literature. Hence, the addition of unknown phase and amplitude parameters in the channel model does not change the fundamental bounds for delay estimation. Also note that the (3,3) element is proportional to $\frac{\langle\tilde{\omega}^2\rangle}{\langle\omega^2\rangle-\langle\omega\rangle^2}$, which is typically a large quantity since the numerator is proportional to ω_c^2 and the denominator is the mean squared bandwidth of the signal which is not a function of ω_c. The (1,3) and (3,1) off-diagonal elements may also be large. This motivates the reparameterization as discussed below.

Reparameterization

In this section, we derive the Fisher information matrix and Cramer-Rao lower bound for a reparameterized representation of the original problem. Let

$$\nu = \phi - (\omega_c + \langle\omega\rangle)\tau \tag{9}$$

and let the new parameter vector be $\boldsymbol{\theta} = [\tau, a, \nu]^\top$. With this parameterization, the mean vector of the whitened observation $\boldsymbol{r}$ can be written as

$$\begin{aligned}\boldsymbol{\mu}(\boldsymbol{\theta}) &= a\exp(-j(\omega_c\tau - \nu - (\omega_c + \langle\omega\rangle)\tau))\boldsymbol{b}(\tau) \quad (10)\\ &= a\exp(j(\langle\omega\rangle\tau + \nu))\boldsymbol{b}(\tau) \quad (11)\end{aligned}$$

The partial derivatives with respect to each unknown parameter can be computed as

$$\begin{aligned}\frac{\partial\boldsymbol{\mu}(\boldsymbol{\theta})}{\partial\tau} &= -ja\exp(j(\langle\omega\rangle\tau + \nu))\left(\mathcal{W}\boldsymbol{b}(\tau) - \langle\omega\rangle\boldsymbol{b}(\tau)\right)\\ \frac{\partial\boldsymbol{\mu}(\boldsymbol{\theta})}{\partial a} &= \exp(j(\langle\omega\rangle\tau + \nu))\boldsymbol{b}(\tau)\\ \frac{\partial\boldsymbol{\mu}(\boldsymbol{\theta})}{\partial\nu} &= ja\exp(j(\langle\omega\rangle\tau + \nu))\boldsymbol{b}(\tau).\end{aligned}$$

where $\mathcal{W}$ again denotes the "frequency operator" consistent with [12].

The calculation of the elements of the Fisher information matrix is similar to the original parameterization. The only elements that change are the $(1,1)$ element and the $(1,3)$ and $(3,1)$ elements. For the $(1,1)$ element, we can compute

$$I_{1,1} = 2a^2\left(\mathcal{W}\boldsymbol{b}(\tau) - \langle\omega\rangle\boldsymbol{b}(\tau)\right)^H\left(\mathcal{W}\boldsymbol{b}(\tau) - \langle\omega\rangle\boldsymbol{b}(\tau)\right)$$

This is of a similar form as the original parameterization except ω_c has been replaced by $\langle\omega\rangle$ and there is a new negative sign to account for in the calculations. The four terms are

$$\begin{aligned}T_1 &= 2a^2\left(\mathcal{W}\boldsymbol{b}(\tau)\right)^H\left(\mathcal{W}\boldsymbol{b}(\tau)\right)\\ T_2 &= -2a^2\langle\omega\rangle\left(\mathcal{W}\boldsymbol{b}(\tau)\right)^H\boldsymbol{b}(\tau)\\ T_3 &= -2a^2\langle\omega\rangle\boldsymbol{b}^H(\tau)\mathcal{W}\boldsymbol{b}(\tau)\\ T_4 &= 2a^2\langle\omega\rangle^2\boldsymbol{b}^H(\tau)\boldsymbol{b}(\tau).\end{aligned}$$

Following the same steps as with the original parameterization, we have

$$\begin{aligned}T_1 &= 2a^2\mathcal{E}_b\langle\omega^2\rangle\\ T_2 &= -2a^2\mathcal{E}_b\langle\omega\rangle^2\\ T_3 &= -2a^2\mathcal{E}_b\langle\omega\rangle^2\\ T_4 &= 2a^2\mathcal{E}_b\langle\omega\rangle^2\end{aligned}$$

where the T_1 element is unchanged but the T_2, T_3, and T_4 elements are all changed with respect to the original parameterization. It follows that

$$I_{1,1} = 2a^2\mathcal{E}_b\left(\langle\omega^2\rangle - \langle\omega\rangle^2\right).$$

For the $(1,3)$ and $(3,1)$ elements, we can compute

$$\begin{aligned}I_{3,1} &= 2\mathrm{Re}\left(\frac{\partial\boldsymbol{\mu}^H(\boldsymbol{\theta})}{\partial\nu}\frac{\partial\boldsymbol{\mu}(\boldsymbol{\theta})}{\partial\tau}\right)\\ &= 2a^2\boldsymbol{b}^H(\tau)(\mathcal{W}\boldsymbol{b}(\tau) - \langle\omega\rangle\boldsymbol{b}(\tau))\\ &= -2a^2\mathcal{E}_b\left(\langle\omega\rangle - \langle\omega\rangle\right)\\ &= 0.\end{aligned}$$

The utility of this reparameterization is now evident in that it causes the Fisher information matrix to be diagonal.

Under the reparameterization, the Fisher information matrix can be written as

$$\boldsymbol{I} = \begin{bmatrix}2\rho\beta^2 & 0 & 0\\ 0 & 2\mathcal{E}_b & 0\\ 0 & 0 & 2\rho\end{bmatrix}$$

where we have used the fact that the mean square bandwidth $\beta^2 = \langle\omega^2\rangle - \langle\omega\rangle^2$. Since the Fisher information matrix is diagonal, the Cramer-Rao lower bound can easily be computed as

$$\mathrm{cov}\left[\hat{\boldsymbol{\theta}}\right] \geq \boldsymbol{I}^{-1} = \begin{bmatrix}1/(2\rho\beta^2) & 0 & 0\\ 0 & 1/(2\mathcal{E}_b) & 0\\ 0 & 0 & 1/(2\rho)\end{bmatrix}. \tag{12}$$

Note that the $(1,1)$ element of the Cramer-Rao lower bound under the reparameterization is identical to the $(1,1)$ element of the Cramer-Rao lower bound under the original parameterization and (1). The $(2,2)$ element is also unchanged. The key difference here is that the Cramer-Rao lower bound is now conveniently diagonal and that the $(3,3)$ element is now much smaller than the $(3,3)$ element of the original parameterization.

This CRLB provides insight into waveform design to achieve desired PTTR performance targets.

5. MAXIMUM LIKELIHOOD PARAMETER ESTIMATION

MLE Derivation

In the previous section, it was notionally convenient to work with the pre-whitened signals $r(t)$ and $b(t)$ and assume the pre-whitened reference signal $b(t)$ had unit energy. In developing an estimation algorithm, we work rather with the original signals $\tilde{r}(t)$, $\tilde{b}(t)$ and do not assume the reference signal to be unit energy. We assume the complex additive Gaussian noise to be wide-sense stationary with a known power spectral density. Use the reparameterization of the channel by (τ, a, ν), where the continuous-time and continuous-frequency unwhitened continuous time observations are given as

$$\tilde{r}(t) = ae^{j\nu}\tilde{b}(t-\tau)\exp\left(j\langle\omega\rangle\tau\right) + \tilde{n}(t) \tag{13}$$

$$\tilde{R}(\omega) = ae^{j\nu}\exp\left(-j(\omega - \langle\omega\rangle)\tau\right)\tilde{B}(\omega) + \tilde{N}(\omega) \tag{14}$$

where ω represents the baseband angular frequency, $N(\omega)$ is the Fourier transform of the WSS noise process with known power spectral density

$$\sigma^2(\omega) := E\left[|N(\omega)|^2\right], \tag{15}$$

$\langle\omega\rangle$ is the mean frequency of the whitened baseband signal

$$\langle\omega\rangle = \int_\omega \omega \frac{|\tilde{B}(\omega)|^2}{\sigma^2(\omega)}\mathrm{d}\omega \Bigg/ \int_\omega \frac{|\tilde{B}(\omega)|^2}{\sigma^2(\omega)}\mathrm{d}\omega\ , \tag{16}$$

Let $\tilde{r}_k, \tilde{b}_k$ denote the discrete-time samples from (**??**). The coefficients of the discrete Fourier transform are

$$\tilde{B}_\ell = \sum_{k=1}^{M_b} \tilde{b}_k \exp\left(-2\pi jk\ell/M\right) \tag{17}$$

$$\tilde{R}_\ell = \sum_{k=1}^{M_r} \tilde{r}_k \exp\left(-2\pi jk\ell/M\right) \tag{18}$$

where $M \geq M_b + M_r - 1$. The lth frequency sample now corresponds to the baseband angular frequency

$$\begin{aligned}\omega_\ell &= \frac{2\pi\ell}{MT} \text{ for } 0 \leq \ell < M/2 \\ &= \frac{2\pi(M-\ell)}{MT} \text{ for } M/2 \leq \ell < M.\end{aligned}$$

If T satisfies the Shannon-Nyquist sampling rate to avoid aliasing given the bandwidth of $\tilde{b}(t)$ and noise bandwidth of $\tilde{n}(t)$, then $\tilde{B}_\ell = \tilde{B}(\omega_\ell)$ and $\tilde{R}_\ell = \tilde{R}(\omega_\ell)$ and (14) becomes

$$\tilde{R}_\ell \approx a e^{j\nu} \exp\left(-j(\omega_\ell - \langle\omega\rangle)\tau\right) \tilde{B}_\ell + \tilde{N}_\ell$$

where the $\tilde{N}_\ell$'s are approximately independent, zero-mean complex Gaussian random variables with $E[|\tilde{N}_\ell|^2] \approx \sigma_\ell^2 = \sigma^2(\omega_\ell)$. Applying Parseval's theorem, the relevant waveform properties can be computed from the frequency-domain reference signal samples and PSD as

$$\mathcal{E}_b = \sum_{\ell=0}^{M-1} \frac{|\tilde{B}_\ell|^2}{\sigma_\ell^2} \tag{19}$$

$$\langle\omega\rangle = \frac{1}{\mathcal{E}_b} \sum_{\ell=0}^{M-1} \omega_\ell \frac{|\tilde{B}_\ell|^2}{\sigma_\ell^2} \tag{20}$$

$$\langle\omega^2\rangle = \frac{1}{\mathcal{E}_b} \sum_{\ell=0}^{M-1} \omega_\ell^2 \frac{|\tilde{B}_\ell|^2}{\sigma_\ell^2} \tag{21}$$

$$\beta^2 = \langle\omega^2\rangle - \langle\omega\rangle^2. \tag{22}$$

Defining $s_\ell(\tau, a, \nu) = a e^{j\nu} \exp\left(-j(\omega_\ell - \langle\omega\rangle)\tau\right)$, the likelihood function can then be written as

$$L(\tau, a, \nu) = \prod_{\ell=0}^{M-1} \frac{1}{\pi\sigma_\ell^2} \exp\left(-\frac{|\tilde{R}_\ell - s_\ell(\tau, a, \nu)\tilde{B}_\ell|^2}{\sigma_\ell^2}\right).$$

The maximum likelihood estimate of the parameter vector $(\hat{\tau}, \hat{a}, \hat{\nu})$ is the argument that maximizes this likelihood. The log likelihood ratio of the signal-present and signal-absent distributions is

$$\gamma(\tau, a, \nu) = \ln\left(L(\tau, a, \nu)/L(*, 0, *)\right) \tag{23}$$

$$= 2a\mathrm{Re}\left(e^{-j\nu} e^{j\langle\omega\rangle\tau} \underbrace{\sum_{\ell=0}^{M-1} \frac{\tilde{R}_\ell \tilde{B}_\ell^*}{\sigma_\ell^2} e^{j\omega_\ell\tau}}_{g(\tau)}\right) - a^2\mathcal{E}_b \tag{24}$$

and is a simpler function with the same maximizing parameters. The values of a and ν maximizing γ are closed-form functions of τ

$$\hat{a}(\tau) = |g(\tau)|/\mathcal{E}_b, \tag{25}$$

$$\hat{\nu}(\tau) = \mathrm{angle}(e^{-j\langle\omega\rangle\tau} g(\tau)). \tag{26}$$

which when substituted into (23) and simplified give

$$q(\tau) = \gamma(\tau, \hat{a}(\tau), \hat{\nu}(\tau)) \tag{27}$$

$$= \frac{|g(\tau)|^2}{\mathcal{E}_b} \tag{28}$$

thus

$$\hat{\tau} = \mathrm{argmax}\left(q(\tau)\right) \tag{29}$$

$$\hat{a} = |g(\hat{\tau})|/\mathcal{E}_b, \tag{30}$$

$$\hat{\nu} = \mathrm{angle}(e^{-j\langle\omega\rangle\hat{\tau}} g(\hat{\tau})). \tag{31}$$

MLE Computation

The $\hat{\nu}$ and $\hat{a}$ estimates are closed-form functions of $\hat{\tau}$, however the $\hat{\tau}$ estimator requires an optimization step. The function $q(\tau)$ is highly multi-modal, changing over timescales inversely proportional to the bandwidth, so our optimization uses search over a set of coarsely-spaced τ_k's, followed by a Newton-Raphson maximization of $q(\tau)$ in the vicinity of the coarse peak. The first and second derivatives of $q(\tau)$ needed in the N-R iteration are

$$\begin{aligned}\dot{q} &= \frac{2}{\mathcal{E}_b}\mathrm{Re}(g\dot{g}^*) \\ \ddot{q} &= \frac{2}{\mathcal{E}_b}\mathrm{Re}(g\ddot{g}^*) + \frac{2}{\mathcal{E}_b}|\dot{g}|^2 \\ \dot{g} &= j\sum_{\ell=0}^{M-1} \frac{\tilde{R}_\ell \tilde{B}_\ell^*}{\sigma_\ell^2} \omega_\ell e^{j\omega_\ell\tau} \\ \ddot{g} &= -\sum_{\ell=0}^{M-1} \frac{\tilde{R}_\ell \tilde{B}_\ell^*}{\sigma_\ell^2} \omega_\ell^2 e^{j\omega_\ell\tau}\end{aligned}$$

In practice, we have found that the convergence region of the N-R iteration is smaller than the initial coarse-spacing of the τ_k's, so we implemented a hybrid bisection / N-R approach where the step size taken is always the smaller of the two optimization approaches.

CRLB Computation

It is of practical value to not only be able to compute the MLE but also bounds on the accuracy of these directly from the data. The CRLB derived in (12) is not directly computable from the data because involves the unknown integrated SNR ρ. The quantity $g(\sigma)$ for any delay σ is a random variable distributed as

$$g(\sigma) \sim \mathbb{CN}\left(ae^{j\nu}e^{j\langle\omega\rangle\tau}\sum_{\ell=0}^{M-1}\frac{|\tilde{B}_\ell|^2}{\sigma_\ell^2}e^{j\omega_\ell(\sigma-\tau)}, \mathcal{E}_b\right),$$

It follows that $q(\hat{\tau}) = |g(\hat{\tau})|^2/\mathcal{E}_b = \hat{a}^2\mathcal{E}_b = \hat{\rho}$ has a non-central chi-square distribution with two degrees of freedom and non-centrality parameter less than or equal to ρ with equality when $\hat{\tau} = \tau$ As such, it has mean $\rho + 2$ and standard deviation $2\sqrt{\rho+1}$, so with high probability (greater than 97%) we have

$$\rho + 2 - 4\sqrt{\rho+1} < \hat{\rho} < \rho + 2 + 4\sqrt{\rho+1}$$

or equivalently

$$\hat{\rho} + 6 - 4\sqrt{\hat{\rho}+3} < \rho < \hat{\rho} + 6 + 4\sqrt{\hat{\rho}+3}.$$

Defining

$$\hat{\rho}_- = \hat{\rho} + 6 - 4\sqrt{\hat{\rho}+3} \tag{32}$$

$$\hat{\rho}_+ = \hat{\rho} + 6 + 4\sqrt{\hat{\rho}+3} \tag{33}$$

then from (12) we obtain the data-computable estimator bounds

$$E\left[|\hat{\tau}-\tau|^2\right] > \frac{1}{2\hat{\rho}_+\beta^2} \tag{34}$$

$$E\left[|\hat{a}-a|^2\right] \geq \frac{1}{2\mathcal{E}_b} \tag{35}$$

$$E\left[|\hat{\nu}-\nu|^2\right] > \frac{1}{2\hat{\rho}_+} \tag{36}$$

The RMS accuracy of the delay and is thus inversely proportional to the square root of the integrated SNR and to the whitened signal bandwidth. The RMS accuracy of the phase scales inversely with the integrated SNR. The accuracy of the amplitude is a fixed value, inversely proportional to the energy in the whitened reference signal.

Generalized Likelihood Ratio Test

It is also often of practical value to have a statistical test for deciding between the presence or absence of the reference signal in the noisy received signal. The likelihood ratio test maximizes the probability of signal-present categorization (detection) for a given probability of signal-absent miscategorization (false alarm) [14], however the likelihood ratio test requires that the true channel parameters (τ, a, ν) be known. An ad-hoc but widely-used test for distributions with unknown parameters is the generalized likelihood ratio test (GLRT) which substitutes into the likelihood ratio the maximum likelihood values of the unknown parameters. The generalized log likelihood ratio $q(\hat{\tau})$ from (27) is a random variable. It is straightforward to show that it has a non-central chi-square distribution with two degrees of freedom and non-centrality parameter equal to the whitened SNR $\rho = a^2\mathcal{E}_b$, where a is the true amplitude. The cumulative distribution function is given by $Pr(q < \zeta) = 1 - Q_1(\sqrt{\rho}, \sqrt{\zeta})$ where $Q_M(a,b)$ is the Marcum Q function, thus for a given threshold ζ, the probability of correct detection and false alarm are, respectively

$$P_{\text{CD}} = 1 - Q_1(\sqrt{\rho}, \sqrt{\zeta}) \tag{37}$$

$$P_{\text{FA}} = Q_1(0, \sqrt{\zeta}). \tag{38}$$

As above, the correct detection probability is not data-computable from the data since ρ is unknown, but we can utilize the probabilistic bounds on ρ given in (32) to get

$$1 - Q_1(\sqrt{\hat{\rho}_+}, \sqrt{\zeta}) < P_{\text{CD}} < 1 - Q_1(\sqrt{\hat{\rho}_-}, \sqrt{\zeta}) \tag{39}$$

6. Numerical Results

To demonstrate the efficacy of the frequency-domain maximum-likelihood estimator derived in Section 5 with respect to the fundamental bounds developed in Section 4, this section provides numerical results assuming additive white complex Gaussian noise. We assume the baseband signal is given by a Hann-weighted linear frequency modulated complex baseband chirp with duration of 5 μs with bandwidth parameter 50 MHz. A time-domain plot of the reference baseband pulse $b(t)$ is shown in Fig. 4

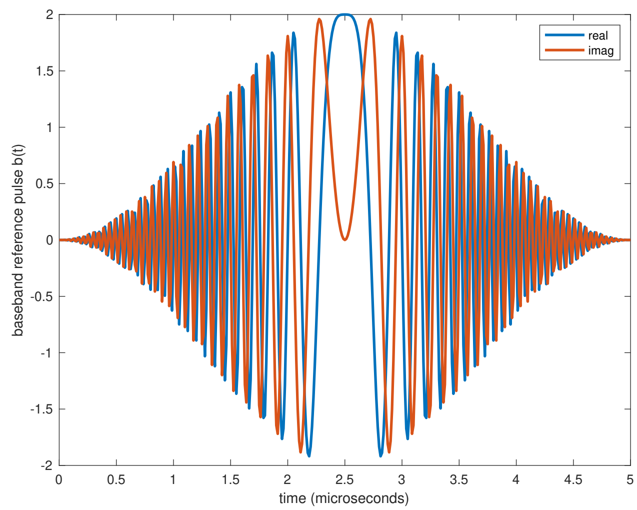

Figure 4. Real and imaginary components of the Hann-weighted linear frequency modulated complex baseband chirp reference pulse $b(t)$ used in this section.

The carrier frequency is further assumed to be 900 MHz. A Monte Carlo simulation was run by generating 20000 independent delay, phase, and noise realizations. Amplitudes were selected deterministically to achieved a specified SNR value. The delay and phase estimation performance results are shown in Figures 5 and 6, respectively.

These results show that, given sufficient integrated SNR, the maximim likelihood estimator is efficient in that the achieved performance closely matches the fundamental limits of the CRLB.

7. Challenges and Future Work

The practical and computationally efficient approach for computing the maximum likelihood estimates of delay, phase and amplitude from a pair of reference and received signals is directly applicable to the system architecture presented in Sec. 2 for obtaining clock synchronization and pairwise ranges between radios in a wireless network network. There are several PTTR challenges that have not been addressed in this paper and will be the subject of future work:

- *Model Limitations:* The three-parameter line-of-sight

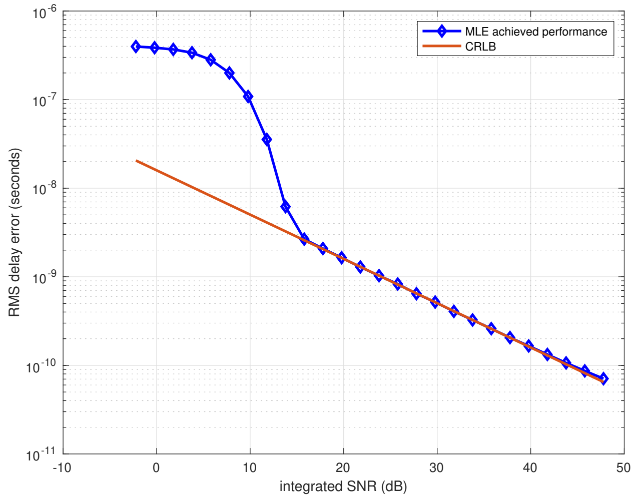

Figure 5. Example of the achieved delay estimation performance of the maximum likelihood estimator versus the Cramer-Rao lower bound.

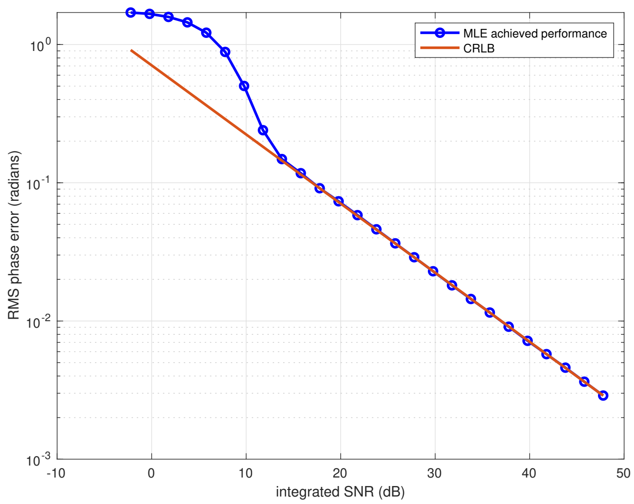

Figure 6. Example of the achieved phase estimation performance of the maximum likelihood estimator versus the Cramer-Rao lower bound.

channel model is simple and captures electronic effects that decouple delay, amplitude and phase. However, multipath in the propagation environment or frequency-dependent electronic group delays may be present and are not captured by this model.

- *Calibration:* The technique allows the total reciprocal component τ^{AB} and anti-reciprocal component ΔT^{AB} to be measured, however a calibration procedure is necessary to remove the non-propagational reciprocal delays in RF cables, electronic components and digital processing to obtain the time-of-flight component. Similar calibration of anti-reciprocal biases are needed to determine the clock offset. These one-time calibration techniques may include loop-back signal collection on individual radios and direct-connection of pairs of radios.
- *Kinematics and Clock Models:* As mentioned, the propagation delay and time offset are stochastic random processes that can be tracked using a Kalman filter, however appropriate state spaces, evolution equations and process noise characteristics of the motion (affecting propagation delay) and clock divergence (affecting the time offset) must be defined and parametrically characterized.
- *Data Volume:* Our technique requires that portions of outbound and inbound waveforms be captured by the sniffers and that the outbound samples be shared over the data network. For wide bandwidth communications with frequent timeslots, this could stress the data capacity of the transport layer used. In this case, techniques that make use of the waveform structure to compress the outbound signals may be effective.

References

[1] D. H. Lee, "OFDMA uplink ranging for IEEE 802.16e using modified generalized chirp-like polyphase sequences," in *2005 1st IEEE and IFIP International Conference in Central Asia on Internet*, Sep. 2005, p. 5 pp.

[2] M. Morelli, L. Sanguinetti, and H. Poor, "A robust ranging scheme for OFDMA-based networks," *IEEE Transactions on Communications*, vol. 57, no. 8, pp. 2441–2452, Aug. 2009.

[3] P. Bidigare, S. Pruessing, D. Raeman, D. Scherber, U. Madhow, and R. Mudumbai, "Initial over-the-air performance assessment of ranging and clock synchronization using radio frequency signal exchange," in *IEEE Stat. Signal Processing Workshop (SSP)*, Aug. 2012, pp. 273–276.

[4] D.R. Brown III and A.G. Klein, "Precise timestamp-free network synchronization," in *Conf. Inf. Sciences and Systems (CISS2013)*, Mar. 2013.

[5] J. Hodkin, K. Zilevu, M. Sharp, T. Comberiate, S. Hendrickson, M. Fitch, and J. Nanzer, "Microwave and millimeter-wave ranging for coherent distributed RF systems," in *Aerospace Conference, 2015 IEEE*, March 2015, pp. 1–7.

[6] M. Li, S. Gvozdenovic, A. Ryan, R. David, D.R. Brown III, and A. Klein, "A real-time implementation of precise timestamp-free network synchronization," Nov. 2015.

[7] A. Weiss and E. Weinstein, "Fundamental limitations in passive time delay estimation–Part I: Narrow-band systems," *Acoustics, Speech and Signal Processing, IEEE Transactions on*, vol. 31, no. 2, pp. 472 – 486, April 1983.

[8] E. Weinstein and A. Weiss, "Fundamental limitations in passive time-delay estimation–Part II: Wide-band systems," *Acoustics, Speech and Signal Processing, IEEE Transactions on*, vol. 32, no. 5, pp. 1064 – 1078, October 1984.

[9] J. A. Nanzer, M. D. Sharp, and Brown, D. Richard III, "Bandpass signal design for passive time delay estimation," in *2016 50th Asilomar Conference on Signals, Systems and Computers*. IEEE, 2016, pp. 1086–1091.

[10] P. Woodward, *Probability and information theory, with applications to radar*. New York, NY: McGraw-Hill, 1953.

[11] M. I. Skolnik, *Introduction to radar systems*. McGraw-Hill, 2001.

[12] L. Cohen, *Time-Frequency Analysis*. Upper Saddle River, NJ: Prentice Hall, 1995.

[13] G. Strang, *Linear Algebra and Its Applications*. Wellesley, MA: Wellesley-Cambridge Press, 1998.

[14] S. M. Kay, *Fundamentals of Statistical Signal Processing Volume I: Estimation Theory*. Upper Saddle River, NJ: Prentice Hall, 1993.

BIOGRAPHY

Patrick Bidigare *received a B.S. in computer engineering and a Ph.D. in mathematics from the University of Michigan, Ann Arbor, in 1992 and 1997 respectively. His doctoral work was in the area of algebraic combinatorics. He was with the Environmental Research Institute of Michigan (later Veridian and General Dynamics) from 1991-2007 and then a technical director at BBN Technologies (later Raytheon) from 2007-2018. Pat led programs in compact multi-static radar systems, quantum sensing, secure communications, coherent distributed communications, distributed RF navigation and timing, and distributed emitter localization. Pat left BBN in 2018 to co-found Synoptic Engineering. Pat's professional interests include new ways of utilizing physical phenomenology for navigation, communications, and environmental sensing.*

Charlie Obranovich *received his bachelor of computer science degree from Michigan Technological University in 2000. He was a research scientist with Honeywell Technology Center working on programs in the areas of wireless sensor networks; acoustic sensing; radio signal processing; industrial controls; and home automation and control. While at Honeywell, Charlie worked in highly distributed teams and led tasking for international colleagues in Germany, India, and the Czech Republic. In 2008, Charlie co-founded a new office for BBN Technologies (later Raytheon BBN Technologies), in St. Louis Park, MN. At BBN, Charlie was principal investigator on DoD programs researching precision time-transfer, ranging, and navigation for airborne and space-borne platforms. In 2020, Charlie joined Synoptic Engineering as managing member.*

David Raeman *received a B.S. degree in computer science from the Georgia Institute of Technology in 2003, and an MBA degree from the University of Maryland in 2010. He was with Harris Corporation from 2003-2007 and then with BBN Technologies (later Raytheon) from 2007-2018 where he provided technical leadership on projects related to distributed coherent transmission, secure communications, and distributed RF navigation and timing. David joined Synoptic Engineering as a managing member in 2020. His professional interests include systems prototyping, resource-limited embedded development, and emerging RF technologies.*

Dan Chang *received a bachelor of science in electric engineering from Case Western Reserve University in 2001 and a master in electrical engineering from the University of Michigan in 2002. He was with General Dynamics (née ERIM) in Ypsilanti, MI from 2002 to 2008 where he served as program manager on secure communication and tagging efforts. From 2008 to 2018 he was a program director at Raytheon BBN Technologies in Arlington, VA where he managed programs in the areas of special communications, radio frequency tagging, distributed communications, distributed beamforming, electronic warfare and positioning, navigation and timing. Dan left Raytheon BBN in 2018 to co-found Synoptic Engineering. Dan's professional interests include maturation of novel concepts into useful capabilities and mentorship.*

D. Richard Brown III *is a Professor in the ECE Department at Worcester Polytechnic Institute. He received the B.S. and M.S. degrees from the University of Connecticut in 1992 and 1996, respectively, and the Ph.D. degree from Cornell University in 2000, all in Electrical Engineering. From 1992 to 1997, he was with General Electric Electrical Distribution and Control. He joined Worcester Polytechnic Institute in 2000 and has also held appointments as a Visiting Associate Professor at Princeton University from 2007 to 2008 and as a Program Director at the National Science Foundation in the Computing and Communication Foundations Division from 2016-2018.*